Journal of Cleaner Production 563 (2026) 148395

Contents lists available at ScienceDirect

Journal of Cleaner Production

journal homepage: www.elsevier.com/locate/jclepro

Upcycling of pyrolytic char waste as a filler for circular asphalt pavement infrastructure

Chai Siah Lee [a,1,2,*], Lu Zhou [b,c,1,2,**], Anand Sreeram [b], Mohamed Adam [a], Ian Cardillo-Zallo [d], Edward Lester [e], Gordon Airey [b], Eleanor Binner [a], Derek Irvine [a]

[a] Faculty of Engineering, University of Nottingham, Nottingham, NG7 2RD, United Kingdom
[b] Department of Civil Engineering, Nottingham Transportation Engineering Centre (NTEC), University of Nottingham, Nottingham, NG7 2RD, United Kingdom
[c] Centre for Engineering Research, School of Physics, Engineering and Computer Science, University of Hertfordshire, Hatfield, AL10 9AB, United Kingdom
[d] Nanoscale & Microscale Research Centre (nmRC), University of Nottingham, Nottingham, NG7 2RD, United Kingdom
[e] Advanced Materials Research Group, Faculty of Engineering, University of Nottingham, Nottingham, NG7 2RD, United Kingdom

HIGHLIGHTS

- First use of poly(methyl methacrylate) pyrolytic char as a sustainable asphalt filler.
- Its mineral and microstructural features support its suitability as a viable filler.
- Replaces up to 75% of limestone while maintaining strong rheological performance.
- Microstructural features of the char yield a balanced binder–filler system in mastics.

GRAPHICAL ABSTRACT

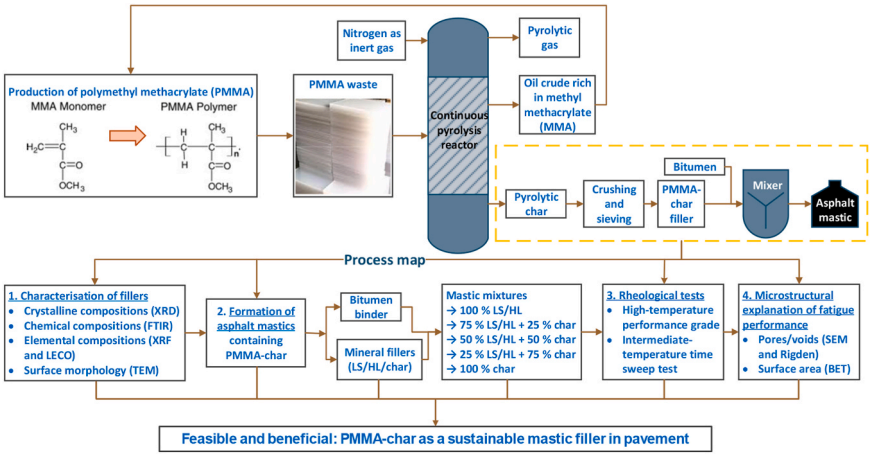

* Corresponding author. Faculty of Engineering, University of Nottingham, Nottingham, NG7 2RD, United Kingdom.
** Corresponding author. Centre for Engineering Research, School of Physics, Engineering and Computer Science, University of Hertfordshire, Hatfield AL10 9AB, UK.
E-mail addresses: chai.lee@nottingham.ac.uk (C.S. Lee), l.zhou7@herts.ac.uk (L. Zhou), anand.sreeram@nottingham.ac.uk (A. Sreeram), mohamed.adam@nottingham.ac.uk (M. Adam), ian.cardillozallo1@nottingham.ac.uk (I. Cardillo-Zallo), edward.lester@nottingham.ac.uk (E. Lester), gordon.airey@nottingham.ac.uk (G. Airey), eleanor.binner@nottingham.ac.uk (E. Binner), derek.irvine@nottingham.ac.uk (D. Irvine).
[1] co-first authors.
[2] These two authors contributed equally to this work.

https://doi.org/10.1016/j.jclepro.2026.148395
Received 16 November 2025; Received in revised form 31 March 2026; Accepted 27 April 2026
Available online 18 May 2026

ARTICLE INFO

Keywords:
Pyrolytic char
Asphalt mastic
Pavement materials
Rheological performance
Waste valorisation
Sustainability
Decarbonisation

ABSTRACT

Incorporating industrial waste into road pavements is a key strategy for advancing asphalt decarbonisation. This manuscript reports the first study into the potential use of a byproduct (defined as PMMA-char) from the industrial pyrolysis of commercial poly(methyl methacrylate) (PMMA) plastic as a sustainable alternative to conventional mineral fillers, namely limestone and hydrated lime, in the asphalt mastic part of an asphalt mixture. Physicochemical characterisation revealed that PMMA-char contained calcite, barium sulfate, and amorphous carbon, exhibiting mineralogical similarities to limestone, which supports its potential as a substitute filler. Various asphalt mastic combinations were prepared by replacing traditional fillers with PMMA-char from 0 to 100% levels, and their rheological properties were evaluated. The overall findings showed that the optimum PMMA-char replacement level depended on the rheological performance metric considered. For limestone-based mastics, the high-temperature Performance Grade (PG) critical temperature peaked at 25–50% replacement, while the fatigue life reached its maximum at 75% replacement. For hydrated lime-based mastics, a 25% replacement level enhanced the high-temperature mastic performance, whereas fatigue life decreased progressively with increasing PMMA-char content. These differences are likely due to variations in microstructure, void ratio, and specific surface area among the fillers, affecting the mastic's effective bitumen fraction. Given that PMMA-char is an industrial byproduct with low economic value, it offers significant promise as a viable low-carbon filler replacement for pavements when compared to current commercial mastic using traditional mineral fillers, which generate significant environmental impact, including high energy consumption, resource depletion, and associated CO_2 emissions.

1. Introduction

Asphalt mixtures, composed of aggregates, bitumen, and mineral fillers such as limestone, are widely used for road construction but are highly carbon-intensive. Producing crushed limestone alone emits about 3.04 kg CO_2e per tonne (Kittipongvises, 2017), excluding additional emissions from processing it into filler. Overall, asphalt pavement uses in the UK generated an estimated 77,300 tonnes CO_2e in 2020 (Wright and Parajuli, 2024), highlighting the significant environmental impact of road materials.

Recognising this impact, National Highways UK has set an ambitious target to achieve net-zero greenhouse gas emissions in construction and maintenance activities by 2040. Its report '*Net Zero Highways: Our Zero-Carbon Roadmap for Concrete, Steel, and Asphalt*' highlights the importance of adopting lower-carbon materials and technologies as key strategies for asphalt decarbonisation. One promising approach to decarbonising asphalt pavements lies in reducing reliance on energy-intensive raw materials, such as mineral fillers, by incorporating industrial by-products or waste synthetic residues. This not only offers a measure to reduce greenhouse gas emissions associated with material production and processing, but it also contributes to more sustainable resource use by promoting circular economy principles.

Recent studies have demonstrated the feasibility of using plastic waste, such as polyethylene, polyethylene terephthalate, and polypropylene, as modifiers to enhance bitumen performance (Hao et al., 2024; Leng et al., 2018). This approach promotes 'circularity' in road construction through effective waste material recycling. However, these materials generally constitute only 5-10% of the binder weight (Sasidharan et al., 2019), and the binder itself typically constitutes about 5% of the total mastic mixture (Pipintakos et al., 2024). Therefore, the overall plastic material content in the final asphalt mixture remains as low as 0.25-0.5%. This relatively low addition level reduces the environmental and economic benefits of large-scale waste plastic reuse.

In contrast, fillers typically represent 4-8% of the total asphalt mixture by weight (Chen et al., 2022). Thus, replacing conventional limestone fillers with calcium carbonate-rich industrial waste materials can offer significant economic and environmental benefits, whilst addressing the increasing concerns regarding the environmental and social impacts associated with limestone extraction. Recent research has focused on incorporating industrial waste materials, such as zinc production waste (Taherkhani and Vahabi Kamsari, 2020), construction and demolition waste, fly ash, jet grouting waste (Russo et al., 2022b), bottom ash (Russo et al., 2022a) and iron tailings (Li et al., 2025) to partially or fully replace limestone in the asphalt mastic part of an asphalt mixture.

In addition to these specific waste materials, pyrolytic char, a byproduct from the plastic recycling pyrolysis process (a form of "chemical recycling"), also presents potential as a sustainable filler in asphalt mixtures. Calcium carbonate/calcite ($CaCO_3$) is commonly added to plastics during industrial manufacturing to improve their stiffness and processability at a low cost (Santos et al., 2023). Since the decomposition of $CaCO_3$ occurs only at elevated temperatures (>700 °C) (Karunadasa et al., 2019), plastic pyrolysis processes typically result in a significant residual $CaCO_3$ content in the resulting char. Considering that limestone is predominantly composed of $CaCO_3$, pyrolytic char containing high $CaCO_3$ content presents a promising alternative to traditional limestone filler.

Among plastics suitable for pyrolysis, PMMA is a promising candidate due to its wide industrial use in aerospace, automotive, construction, medical, and coating applications, and its key properties of high transparency and glass transition temperature. It is lightweight, electrically insulating, and corrosion-resistant (Ding et al., 2022). Global PMMA production reached 3.9 million tonnes in 2022 and is projected to grow at 3.4% annually, yet only about 10% is recycled (Sponchioni and Altinok, 2022a; Young et al., 2023), creating significant environmental challenges.

Pyrolysis, a widely recognised method for chemical recycling of polymers, holds particular promise for PMMA plastic, because it undergoes molecular decomposition (i.e. depolymerisation via main chain bond scission) when heated, yielding a liquid crude rich in methyl methacrylate (MMA) monomer, which can be reused to produce new high-performance PMMA plastic. This is a superior recycling method compared with "mechanical reuse" methods, where the subsequent products typically exhibit reduced performance compared to the original structure. However, in addition to the monomer, a pyrolytic char by-product (designated as PMMA-char in this study) is also generated (Braido et al., 2018; Gkaliou et al., 2023). Prior literature reporting the pilot-scale PMMA plastic pyrolysis processes has defined yields of liquid crude monomer and PMMA-char ranging from 64.9 to 96.7 *wt*% and 0.1-27.3 *wt*%, respectively, depending on the additives or fillers in the PMMA plastic and the processing conditions (Braido et al., 2018; Kaminsky and Eger, 2001; Ribeiro et al., 2024). Currently, PMMA-char has limited industrial applications and is often discarded in landfills, representing a missed opportunity to reduce the environmental impacts associated with PMMA plastic waste.

This study supports the UK's net-zero and circular economy goals by exploring PMMA-char as a sustainable alternative to traditional mineral fillers, such as limestone, in asphalt mastics. It investigates the feasibility

and performance benefits of using PMMA-char, which contains $CaCO_3$, as a value-added filler. A process map highlighting this focus (yellow dashed section) is shown in Fig. 1.

2. Materials and methods

2.1. Materials

2.1.1. Bitumen

A neat bitumen with a penetration of 70/100 (B70/100) was used to prepare the asphalt mastics, and their main properties are presented in Table S1 in the Supplementary Information (SI).

2.1.2. Fillers

In this study, the asphalt mastic fillers included PMMA-char and two conventional fillers, limestone and hydrated lime, as shown in Fig. S1. The PMMA-char, supplied by Mitsubishi Chemical UK, was a by-product from a PMMA pyrolytic recycling facility operating at a processing temperature of 430-450 °C (feedstock grade undisclosed). The received char particles (a few millimetres to 1 cm) were ground with a pestle and mortar and sieved to below 75 μm, the standard filler size (Sponchioni and Altinok, 2022a). Limestone and hydrated lime fillers (<75 μm) were obtained from Buxton Lime and Acros Organics, respectively.

2.1.3. Asphalt mastic preparation

Bitumen was heated to 150 °C for proper fluidity, and filler was added at a 1:1 filler-to-bitumen ratio. The mixture was stirred at 200 rpm for 20 min at 150 °C to ensure uniform dispersion. To assess PMMA-char as a filler substitute, it was blended in varying proportions to replace limestone and hydrated lime, as shown in Table S2. All filler substitutions were conducted on a mass basis. It should be noted that, because PMMA-char, limestone, and hydrated lime have different particle densities, identical mass replacement does not correspond to identical filler volume replacement.

2.2. Characterisation methods of fillers

Each filler was characterised by Rigden Voids (RV) test, Brunauer–Emmett–Teller (BET) analysis, Attenuated Total Reflectance Fourier-Transform Infrared (ATR-FTIR) analysis, X-ray Powder Diffraction (XRD) analysis, X-Ray Fluorescence (XRF) analysis, carbon (C) and hydrogen elemental analysis, Transmission Electron Microscopy (TEM) analysis and Scanning Electron Microscopy (SEM) analysis. The details of each method are explained in the SI.

2.3. Rheological performance tests on asphalt mastics

2.3.1. High-temperature performance testing

The high-temperature rheological behaviour of mastics was evaluated using a Dynamic Shear Rheometer (DSR) following AASHTO T 315. Thin mastic samples were tested between 25 mm parallel plates at a 1 mm gap under a constant frequency of 10 rad/s, starting from 76 °C and increasing in 6 °C steps. At each temperature, the complex shear modulus (G^*) and phase angle (δ) were recorded to calculate the rutting factor, $G^*/\sin\delta$, which was used here as a comparative indicator of resistance to permanent deformation. Higher values imply better rutting resistance. The high-temperature performance grade (PG) was defined as the highest temperature at which $G^*/\sin\delta \geq 1.0$ kPa, a binder-based criterion used here only as a common rheological basis for comparing mastic formulations with different PMMA-char replacement levels under identical test conditions, since no standard exists for mastics. The derived critical temperatures were used as relative comparative indicators of high-temperature rheological performance, rather than as formal PG classifications for mastics. All tests were performed in duplicate for reliability.

2.3.2. Time sweep fatigue performance testing

The fatigue performance of asphalt mastics was assessed using a DSR with 8 mm plates and a 2 mm gap at 25 °C, applying 2% strain at 10 Hz. The test continued until the complex shear modulus (G^*) decreased by 50%, defining failure (Hyun-Jong et al., 2000). The corresponding number of cycles (N_f) was used as a relative indicator of rheological fatigue resistance under the selected test conditions, with higher N_f values indicating better fatigue tolerance within this comparative framework. It should be noted that this testing approach was used to enable like-for-like comparison among mastics with different PMMA-char replacement levels, rather than to provide a direct prediction of mixture- or pavement-scale fatigue performance. Each sample was tested in triplicate for reliability.

3. Results and discussion

This study evaluates the feasibility of employing PMMA-char as an alternative filler to those fillers traditionally used in asphalt mastics. The study included: (1) a systematic comparison of the crystallinity, crystal structure, chemical composition, and surface morphology exhibited by PMMA-char and conventional control fillers (limestone and hydrated lime) and (2) the preparation and property evaluation of asphalt mastics by partially substituting limestone filler or hydrated lime filler with PMMA-char at various replacement levels. Consequently. it presents a

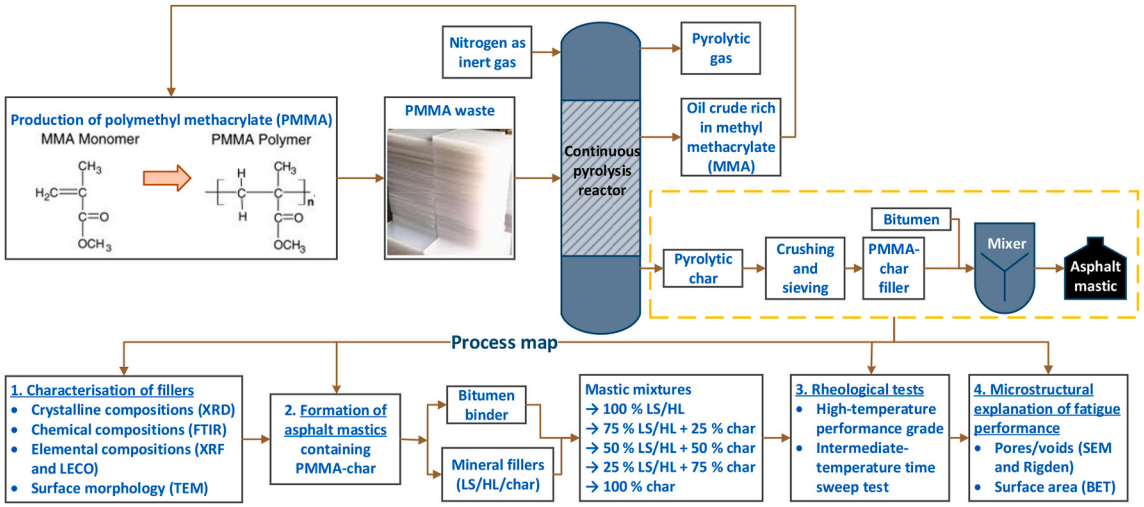

Fig. 1. Process map of this study. (Notes: LS = limestone, HL = hydrated lime).

pathway to reducing both the carbon footprint of asphalt mastics and contributing to the economic viability of decarbonisation in the PMMA recycling process.

3.1. Characterisation and comparison of physicochemical properties of fillers

3.1.1. Crystalline Compound(s) via XRD analysis

The XRD patterns of the PMMA-char, limestone, and hydrated lime fillers are presented in Fig. 2(a), whilst the crystallinity and crystal structure of the detected compounds computed from the XRD pattern of each filler are listed in Table S3.

The XRD analysis revealed that both limestone and hydrated lime are highly crystalline materials with crystallinity levels of >84% (Table S3). The crystalline phases in limestone consist of calcite, dolomite and quartz, whilst hydrated lime contains portlandite, consistent with the results reported in the literature (Chen et al., 2022; Zhao et al., 2021).

Meanwhile, the analysis of the XRD pattern of PMMA-char (Table S3) indicates that it is a semi-crystalline material, comprising both crystalline (53%) and amorphous (47%) regions. Its crystalline phases contain calcite and barium sulfate. This was expected because calcite is commonly used as a filler in PMMA manufacturing to enhance abrasion resistance, thermal stability, and optical performance of PMMA plastic (Avella et al., 2001; Elimat et al., 2008). Meanwhile, barium sulfate is widely employed as a radio-opacifying agent in the commercial formulation of PMMA (Miola et al., 2023). Furthermore, these two compounds are thermally stable, with their thermal decomposition taking place at high temperatures between 700 and 800 °C (Karunadasa et al., 2019) for calcite and between 1400 and 1600 °C for barium sulfate (Holt and Engelkemeir, 1970). This is far beyond the typical pyrolysis processing temperatures used in depolymerising PMMA to its monomer, which are typically in the region of 400-450 °C (Chin et al., 2024; Gkaliou et al., 2023), which explains the presence of calcite and barium sulfate in the PMMA-char by-product.

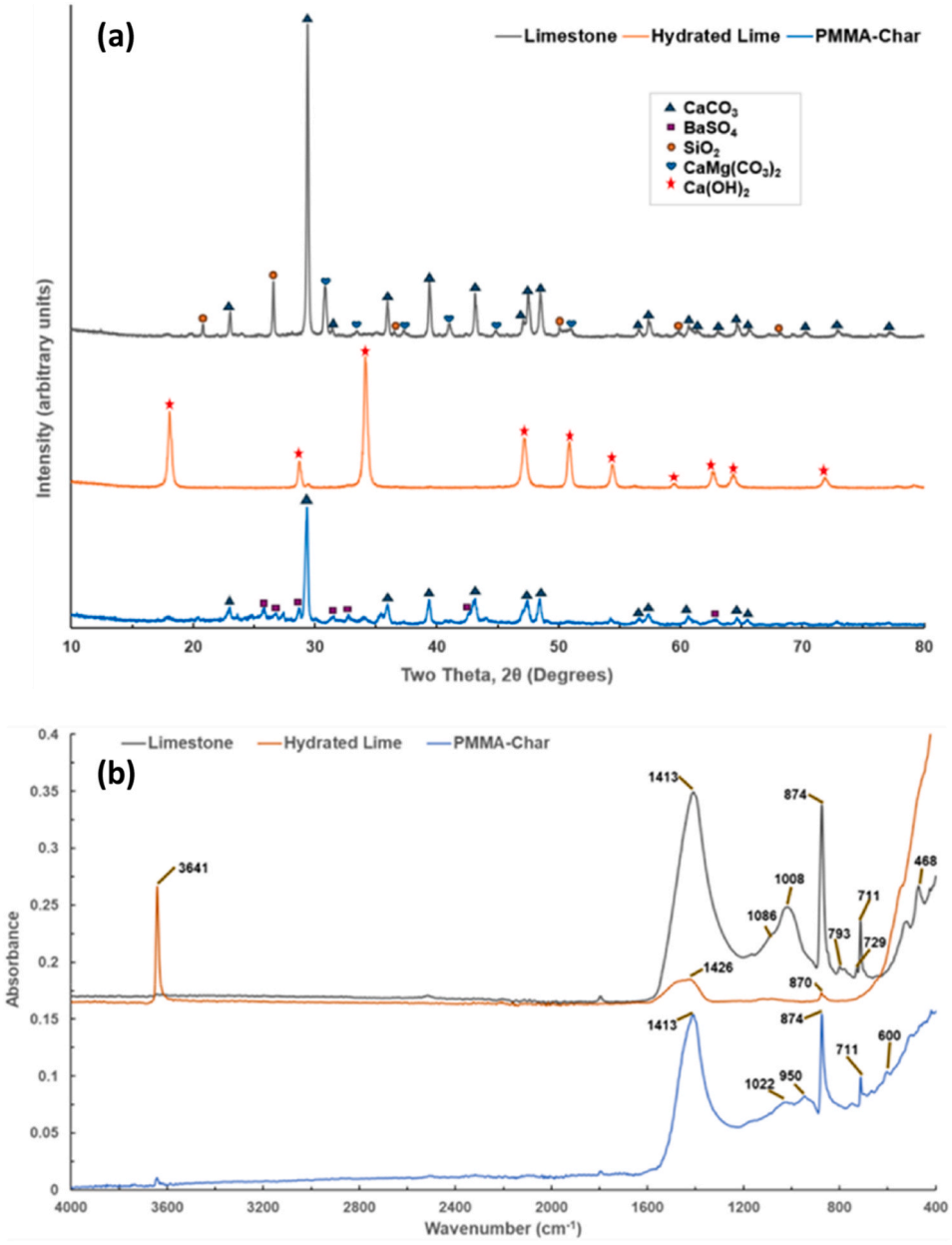

Fig. 2. (a) XRD patterns of the PMMA-char, limestone, and hydrated lime fillers (Notes: $CaCO_3$ = calcium carbonate/calcite, $BaSO_4$ = barium sulfate, SiO_2 = quartz, $CaMg(CO_3)_2$ = dolomite, $Ca(OH)_2$ = portlandite) and (b) the FTIR spectra of limestone, hydrated lime and PMMA-char fillers.

The amorphous phase in PMMA-char is anticipated to be the carbon-based material, which is the common char material formed during the polymer pyrolysis process (Lawson and Srivastava, 2008). This is expected as the parent material is predominantly organic polymer PMMA. Through carbon and hydrogen elemental analysis, the PMMA-char was found to contain 53.08 ± 0.36 *wt*% carbon and 1.52 ± 0.15 *wt*% hydrogen.

The XRD patterns also showed that the calcite diffraction peaks from PMMA-char align with those in the limestone filler, indicating that the calcite in both samples is present in a rhombohedral crystal structure. Moreover, in terms of acid-base characteristics, PMMA-char, similar to limestone fillers, exhibits a weak alkaline nature, which may be beneficial for forming a strong adhesive bond with bitumen binder, a mildly acidic material under dry conditions (Mihandoust and Ghabchi, 2025; Yang et al., 2024; Zhou et al., 2024). However, its bond durability under wet conditions remains to be verified experimentally. These preliminary findings supported the potential feasibility of using PMMA-char as a substitute for conventional fillers, particularly limestone.

3.1.2. Chemical bonds and compound(s) via FTIR analysis

The FTIR spectra of the three fillers are presented in Fig. 2(b), and the assignment of each band is summarised in Table S4. The comparison of the FTIR spectra of PMMA-char and limestone confirmed that both char and limestone contained mainly calcite, as three sharp characteristic bands associated with calcite at 1413 (high-intensity band), 874, and 711 cm^{-1} were detected. In addition to calcite, the PMMA-char's spectrum displayed three bands linked to the presence of barium sulfate at 1022, 950, and 600 cm^{-1}. Additionally, the limestone's spectrum showed bands corresponding to the presence of dolomite (1413, 874, and 729 cm^{-1}) and quartz (1086, 1008, 793, and 468 cm^{-1}).

In contrast, the spectrum of hydrated lime was relatively simple with three bands at 3641, 1426, and 870 cm^{-1}, which were associated with the presence of portlandite. The strong O-H stretching band at 3641 cm^{-1} is the characteristic band for portlandite. A broad band at 1426 cm^{-1} and a weak band at 870 cm^{-1} are the absorption peaks linked to amorphous calcium carbonate, which was anticipated to be the product formed due to the reaction between carbon dioxide in the atmosphere and portlandite (lime carbonisation) (Cizer et al., 2012).

3.1.3. Chemical elements via XRF analysis

The fillers were then further analysed with XRF analysis to identify the elemental composition of each filler. The identification and quantification of elements provide a good indication of the possible compounds in each filler, and the elemental content can be used to calculate the chemical compositions. The results are presented in Table S5, which further supports the conclusions drawn above from the XRD and FTIR analyses. Specifically, the XRF data verified the abundance of calcium in the hydrated lime, which is likely derived from portlandite. Limestone was found to contain calcium as the major element, followed by silicon and magnesium as the minor elements, indicating the presence of calcite, dolomite, and quartz in limestone.

Furthermore, the chemical compositions of both hydrated lime and limestone were calculated based on their elemental content (refer to the example calculation below Table S5). The results revealed total compositions of 99.58 *wt*% for hydrated lime and 99.65 *wt*% for limestone. The remaining 0.42 *wt*% in hydrated lime and 0.35 *wt*% in limestone are likely corresponding to trace amounts of silicon dioxide and magnesium oxide, respectively (Chen et al., 2022; Zhao et al., 2021)) which were below the detection limits of the analytical techniques employed in this study.

XRF analysis of PMMA-char showed that it consists of calcium as the major element and barium as the minor element, further supporting the presence of calcite and barium sulfate in PMMA-char. The calculated chemical compositions for PMMA-char indicated 43.58 *wt*% calcite and 0.65 *wt*% barium sulfate, yielding a total of 44.23 *wt*%. The remaining fraction is presumed to be amorphous carbon, consistent with the observations discussed in Section 3.1.1. Although barium sulfate is a rigid and stable inorganic phase, its content in PMMA-char is very low (0.65 *wt*% based on XRF analysis), suggesting that its contribution is likely secondary relative to the dominant calcite-rich mineral fraction and the amorphous carbonaceous phase.

3.1.4. Microstructure and surface morphology via TEM analysis

The structure and morphology of individual particles of limestone, hydrated lime, and PMMA-char fillers were analysed by bright-field TEM imaging, presented in Fig. 3.

As shown in Fig. 3, particle agglomeration was observed across all fillers on the carbon support film, which hindered the identification of distinct particle boundaries, although it is noted that some individual particles could be identified, particularly for hydrated lime filler.

Despite the agglomeration and clustering observed, TEM imaging revealed faceted particles exhibiting diffraction contrast, demonstrating the presence of crystallinity within each filler. In the case of limestone filler powder (Fig. 3(a and b)), this observation, coupled with XRD findings, suggests the presence of a rhombohedral crystal structure characteristic of calcite (Roberto et al., 2023), which is the most thermodynamically stable form of calcite at room temperature (Chaiyaput et al., 2022). Similarly, it is proposed that hydrated lime filler powder, as depicted in Fig. 3(c and d), exhibits a hexagonal crystalline structure (Bahraq et al., 2022; Mouillet et al., 2014) as identified by XRD analysis.

TEM imaging of PMMA-char filler (Fig. 3(e and f)) similarly reveals a crystalline material, particularly evident in Fig. 3(f), while XRD observations suggest the presence of both crystalline calcite and barium sulfate. In addition, a significant presence of an amorphous material is noted, exemplified by areas in Fig. 3(e, upper and lower sections) and Fig. 3(f, upper section).

3.2. Rheological properties of asphalt mastics: performance justification

3.2.1. Comparison of high-temperature performance of asphalt mastics at various blending ratios

Fig. 4 presents the temperature-dependent variation in rutting factors of asphalt mastic samples, in which limestone filler (Fig. 4(a)) and hydrated lime filler (Fig. 4(b)) were replaced by PMMA-char at various replacement rates (as shown in Table S2). The critical temperatures derived from the binder-based DSR rutting criterion for limestone-based and hydrated lime-based mastics are summarised in Table 1. In this study, these values are used as comparative indicators to evaluate the relative effect of different PMMA-char replacement levels under a common testing framework, rather than as formal PG classifications for mastics.

Results are averaged from at least three replicates per formulation. With increasing test temperature, the rutting factor of both types of mastics gradually decreases. However, replacing traditional filler with PMMA-char significantly enhances high-temperature rutting resistance within a broad range (76-112 °C), especially at moderate-to-high replacement levels. The limestone-based mastic with a bitumen: PMMA-char: limestone ratio of 50%:37.5%:12.5% (75% replacement ratio) showed the best performance below the performance grade (PG) critical temperature (i.e., the temperature just before the $G^*/sin(\delta)$ value falls below the 1.0 kPa threshold), while the hydrated lime-based mastic performed optimally at a 50% replacement.

However, as the temperature approaches the critical threshold, the bitumen viscoelastic relaxation and the reinforcement effect of high PMMA-char content become less pronounced. Therefore, the high-temperature performance of mastics with different replacement levels tends to converge. As shown in Table 1, for limestone-based mastics, the critical temperature was enhanced from 106 to 112 °C as the char content rose to 50% replacement level, but declined again to 106 °C at higher replacement levels. Similarly, for hydrated lime-based mastics, a 25% replacement level enhanced the critical temperature from 100 to 112 °C, but further increases in char content reduced it to 106 °C. This

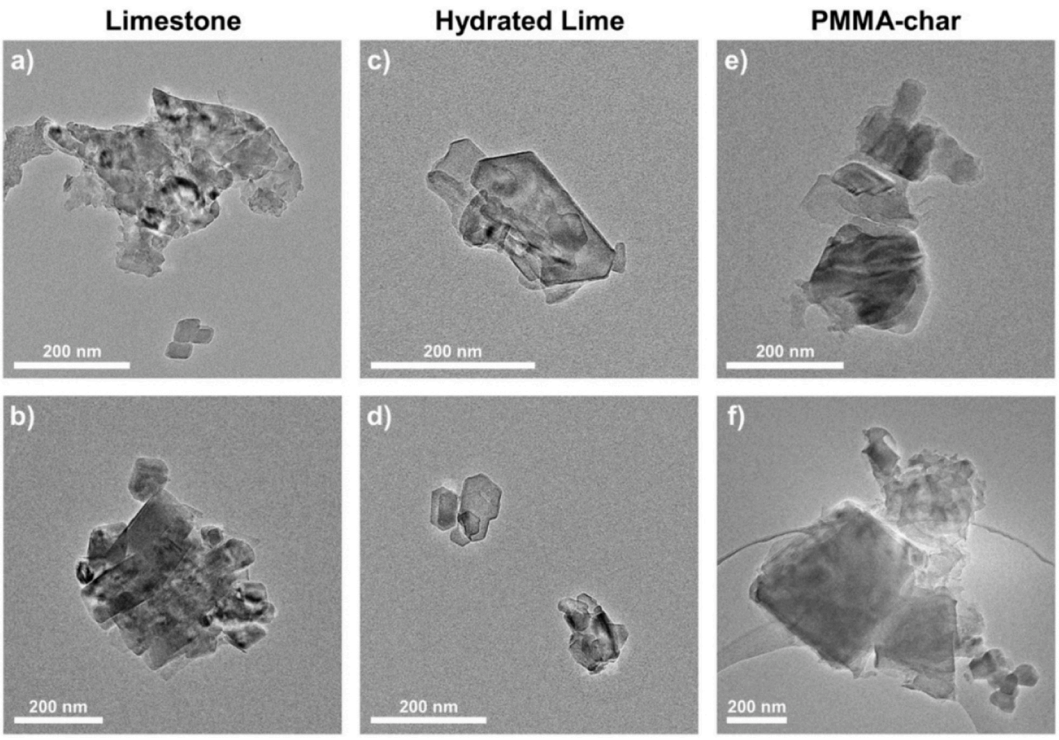

Fig. 3. TEM images of (a,b) limestone, (c,d) hydrated lime, and (e,f) PMMA-char fillers supported on amorphous carbon film.

suggests that while higher PMMA-char content enhances rutting resistance before the critical temperature, the optimal replacement ratio at the PG threshold is lower, approximately 50% for limestone-based and 25% for hydrated lime-based mastics.

This may be attributed to the reinforcing effect of PMMA-char at subcritical temperatures, where its higher angularity and surface roughness promote stronger physical contact with the binder and improve the packing of the filler skeleton (Zhang et al., 2018), leading to a more stable mastic structure. However, as the temperature approaches the PG threshold, the reduction in rutting factor suggests increased binder fluidity and viscous dominance, which may compromise filler skeleton, especially at higher char contents. As a result, the optimal replacement ratio at the critical temperature tends to be lower (25-50%), highlighting the importance of tailoring filler composition not only based on material properties but also on the specific service temperature range of asphalt pavements. In addition, as particle densities differ significantly between PMMA-char and mineral fillers, the associated changes in filler volume fraction are likely to play a role, and this should be considered in future studies.

3.2.2. Comparison of rheological fatigue performance of asphalt mastics at various blending ratios

The Time Sweep Fatigue test was conducted to provide a comparative assessment of the intermediate-temperature fatigue performance of the two types of asphalt mastics with different PMMA-char replacement levels at 25 °C. The results are shown in Fig. 4(c). Overall, the limestone-based mastic without PMMA-char exhibited lower fatigue performance compared to the hydrated lime-based mastic, possibly due to the chemical interactions at the filler–bitumen interface. In mastics, limestone primarily functions as an inert stiffening filler with weakly polar calcite surfaces, and the adhesion between the filler and bitumen relies mainly on van der Waals forces (Bhasin et al., 2008). In contrast, hydrated lime is strongly alkaline and can react with acidic functional groups in bitumen to form stable calcium-carboxylate ("Ca-soap") complexes, which enhance both the stiffness and moisture resistance of mastics (Kandhal and Chakraborty, 1996; Little and Petersen, 2005). In addition, differences in filler volume fraction between the two mastics may also play a role, as hydrated lime replacement by mass is likely to correspond to a higher filler proportion than limestone. This factor will be considered in more detail in the next section.

As shown in Fig. 4(c), PMMA-char affected the two mastics differently. In limestone-based mastics, fatigue life improved with increasing PMMA-char content, peaking at 75% replacement, but declined at 100%, returning to the baseline level. Conversely, in hydrated lime-based mastics, fatigue life consistently decreased as PMMA-char content increased. The contrasting fatigue responses may be attributed to the mechanical (geometric) interactions governed by void structure, including the variations in the void ratios or surface areas of the limestone, hydrated lime, and PMMA-char fillers [49,50]. To validate this hypothesis and further interpret the rheological results, microstructural characterisation was performed using the SEM, RV, and BET analyses.

3.2.3. Comparison of filler microstructure and mechanistic interpretation of the DSR results

SEM was employed to examine the limestone, hydrated lime, and PMMA-char fillers, providing direct insight into their micropores and particle stacking. Fig. S2 shows the SEM images of the three fillers at 15,000× magnification. It is evident that the limestone filler particles differ markedly from hydrated lime and PMMA-char fillers, presenting a lamellar, densely packed structure with low internal porosity (Dimulescu and Burlacu, 2021). Hydrated lime filler exhibits coralloid-like arrangements and a highly porous structure created during slaking, showing the highest voids (Lesueur et al., 2013). PMMA-char filler contains a carbonaceous matrix riddled with meso-/micro-pores left after polymer pyrolysis. It displays a similar structure to hydrated lime, but with pore size and distribution intermediate between those of limestone (lowest porosity) and hydrated lime (highest porosity).

Subsequently, the Rigden Voids test (two replicates) and BET analysis (three replicates) were performed to evaluate the microstructural characteristics of the three fillers quantitatively. The test results for the volume of voids and specific surface area for each filler are presented in

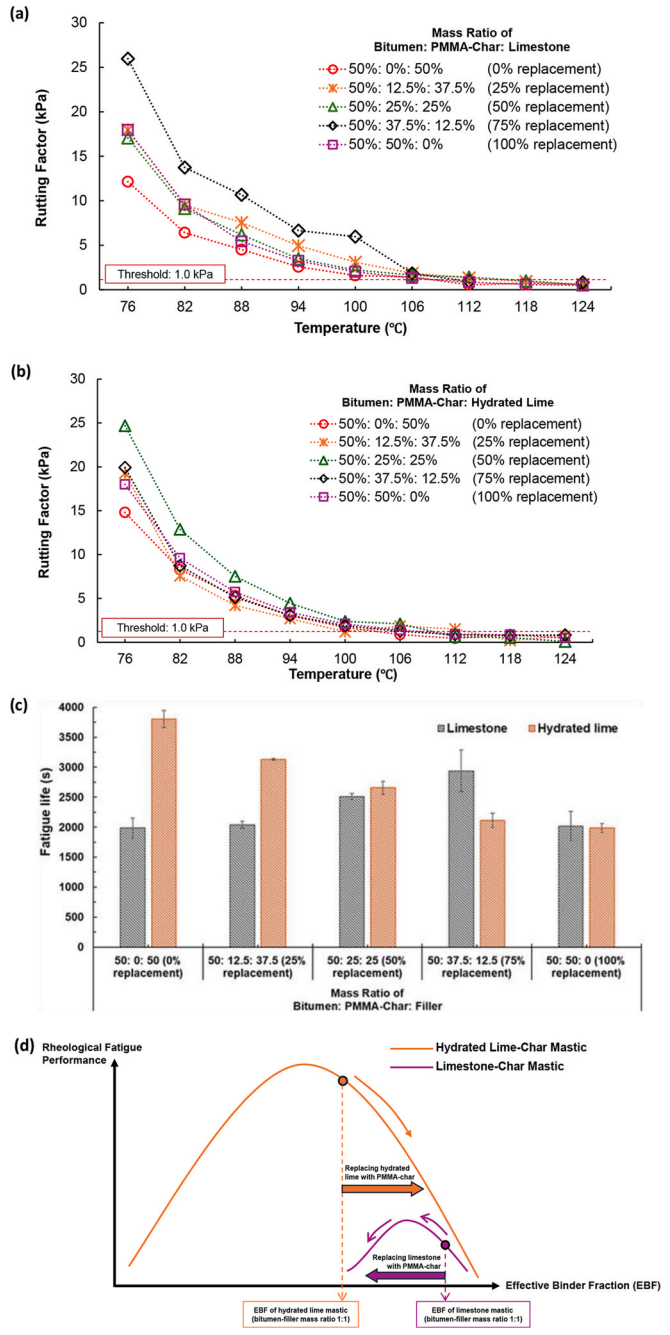

Fig. 4. The rutting factor $G^*/sin(\delta)$ of (a) limestone-based mastics and (b) hydrated lime-based mastics containing PMMA-char with replacement levels from 0 to 100% as a function of temperature, (c) the rheological fatigue life of mastic samples with various blending ratios, and (d) conceptual relationship between EBF and rheological fatigue performance of asphalt mastics with different fillers.

Table S6. The measurements consistently show that limestone has the lowest void content (highest solid packing) and the smallest specific surface area among the three fillers, whereas hydrated lime exhibits the highest values, with PMMA-char falling in between. These microstructural characteristics directly influence the effective binder fraction (EBF), defined as the proportion of bitumen volume remaining free to flow after subtracting the volume needed to fill the inter-particle voids of compacted filler (Rigden Voids). For porous fillers, the inter-particle voids given by the Rigden Voids test do not account for the intra-particle

Table 1
Critical temperature derived from the DSR rutting criterion for limestone-based and hydrated lime-based mastics with various blending ratios.

Asphalt Mastic Mixture	Mass Ratio for Bitumen: PMMA-Char: Filler	PMMA-char Replacement Level (%)	Critical Temperature: High-temperature PG (°C)
Bitumen:	50: 0: 50	0	106
PMMA-	50: 12.5: 37.5	25	112
Char:	50: 25: 25	50	112
Limestone	50: 37.5: 12.5	75	106
	50: 50: 0	100	106
Bitumen:	50: 0: 50	0	100
PMMA-	50: 12.5: 37.5	25	112
Char:	50: 25: 25	50	106
Hydrated	50: 37.5: 12.5	75	106
lime	50: 50: 0	100	106

porosity, which may also absorb binder and reduce the EBF. This effect should be considered separately. At the bitumen-filler mass ratio of 1:1, limestone's compact packing and low surface area require less binder to cover the particles, resulting in a higher EBF in limestone-based mastics (Bryant, 2005; Zhang et al., 2017). In contrast, hydrated lime-based mastics have the lowest EBF due to their high void content and large specific surface area, and higher filler volume fraction arising from their lower particle density. PMMA-char filler (with the Rigden Voids between limestone and hydrated lime fillers) behaves differently depending on the filler it replaces. When substituting limestone, the higher porosity and lower particle density of PMMA-char increase the filler volume fraction and void content, thereby reducing the EBF. When replacing hydrated lime, the same mechanisms are also present, but the effect is likely moderated by the smaller density contrast and the already high porosity of hydrated lime, leading overall to a relative decrease in voids and an increase in EBF. These results suggest that multiple factors, including surface area, intra-particle porosity, and particle density, act simultaneously and influence the net EBF response.

EBF is closely linked to bitumen film thickness, which governs the flowability, adhesion, and durability of asphalt mixtures. Numerous studies report an "optimum zone" for film thickness, typically 6-9 μm for full asphalt mixtures, outside which both durability and fatigue life deteriorate (Li et al., 2020; Lin et al., 2023). For example, previous studies (Bryant, 2005) on stone mastic asphalt (SMA) have adopted free binder limits of 8.0–11.0% for mix design, with extended limits of 7.5–11.0% for production. Similarly, in mastic systems, the effective binder fraction also exhibits an optimum range rather than a monotonic relationship with performance. Insufficient EBF leads to a dry, brittle mastic with poor cohesion, whereas excessive EBF reduces structural stability and decreases fatigue resistance under repeated loading. The exact optimum range varies with filler type.

This concept helps explain the varying rheological fatigue performance trends observed in Fig. 4(c). In limestone-based mastics, increasing PMMA-char leads to a progressive decrease in EBF. This initially improves fatigue life until an optimal point is reached, beyond which performance declines. In hydrated lime-based mastics, PMMA-char replacement is expected to increase EBF. Under the present formulation, this appears to move the system away from the optimum EBF range for fatigue resistance. At the same time, the replacement of hydrated lime also reduces the active filler–bitumen interaction originally provided by hydrated lime. As a result, fatigue performance decreases progressively with increasing PMMA-char content. Fig. 4(d) schematically illustrates the conceptual relationship between bitumen EBF and rheological fatigue behaviour across different filler systems, highlighting that the response is governed by an optimum range rather than a simple monotonic trend. It should be noted that the EBF-based interpretation presented in this study is conceptual and supported qualitatively by the Rigden Voids results. A rigorous quantitative derivation of EBF for porous PMMA-char-containing mastics requires further methodological development and complementary measurements.

In summary, high-temperature performance tests and intermediate-temperature fatigue experiments indicate that PMMA-char can potentially serve as a partial substitute for traditional limestone filler in asphalt mastics, with replacement levels up to 50% showing comparable or improved rheological performance. Based on a global PMMA production of approximately 3.9 million tonnes annually (Sponchioni and Altinok, 2022b), and assuming full recycling via pyrolysis with a 15 *wt*% char yield, an estimated 585,000 tonnes of PMMA-derived char could theoretically be produced each year. If the char is fully utilised as a filler, and assuming a representative filler price of USD 50-70 per tonne, depending on particle size and location (Chen et al., 2020), this could correspond to indicative annual cost savings of USD 30-41 million.

From a sustainability perspective, PMMA-char may offer additional benefits, as it is derived from industrial waste streams and could provide a pathway for valorising PMMA through thermochemical recycling. Its use as a filler may therefore contribute to broader circular economy initiatives in pavement engineering, although the overall environmental benefits would require confirmation through a comprehensive life cycle assessment.

While a detailed life cycle cost analysis (LCCA) is beyond the scope of this study, the observed improvements in fatigue performance of PMMA-char-modified mastics suggest the possibility of enhanced durability. If such improvements translate to asphalt mixtures and pavements at larger scales, they could potentially contribute to longer service life or reduced maintenance interventions. These aspects warrant further investigation through mixture- and structural-level studies.

4. Conclusions

This study investigated the feasibility of using plastic pyrolytic char derived from industrial PMMA waste as a mineral filler substitute in asphalt mastic, evaluated at the laboratory mastic scale and compared with conventional limestone and hydrated lime fillers. The key findings are as follows:

(1) Material characterisation: Limestone and hydrated lime are highly crystalline, comprising mainly calcite and portlandite, respectively. PMMA-char is semi-crystalline, containing calcite, minor barium sulfate, and amorphous carbon, resulting in a mineral composition broadly comparable to limestone.
(2) Rheological performance: Partial replacement of traditional fillers with PMMA-char improved asphalt mastic rheological performance. Replacing 50% of limestone or 25% of hydrated lime enhanced high-temperature behaviour. At intermediate temperatures, fatigue resistance increased with increasing replacement of limestone by PMMA-char, reaching an optimum at 75%, whereas any substitution in hydrated lime-based mastics reduced fatigue resistance.
(3) Microstructural analysis: SEM, BET, and Rigden Voids analyses showed that PMMA-char has intermediate packing characteristics and surface area between limestone and hydrated lime. This corresponds to an effective binder fraction (EBF) that falls between the two reference fillers, providing a balance between binder availability and filler packing that influences rheological behaviour.

Overall, PMMA-char shows promise as a sustainable filler substitute in asphalt mastics, particularly in limestone-based systems, supporting the circular utilisation of plastic-derived pyrolysis char in pavement materials.

5. Future outlook

It should be noted that this study used PMMA-char sourced from a recycling pilot facility, and its potential as a filler substitute was evaluated only at the asphalt-mastic scale. The results do not account for possible variations in PMMA-char composition arising from different PMMA waste streams and additives, which may influence its physical and chemical properties and its interaction with bitumen. In addition, although the compositional analyses suggested that the contribution of barium sulfate is likely limited due to its very low content, the present study did not experimentally isolate the individual effects of the mineral phases and the amorphous carbonaceous phase in PMMA-char. Furthermore, the complex stress, traffic loading, and environmental conditions acting on full asphalt mixtures were not represented, and long-term effects such as ageing, moisture damage, and freeze–thaw cycles were not assessed.

Future work should therefore (i) assess the influence of PMMA-char variability from different feedstocks on mastic performance, (ii) establish quality control requirements for PMMA-char production to ensure consistent properties for asphalt applications, and (iii) extend testing to the asphalt-mixture scale through comprehensive mechanical evaluations (e.g., rheological, rutting, fatigue, and moisture-susceptibility tests). Related follow-up studies at the asphalt-mixture scale are currently underway and will be reported separately. Environmental aspects should also be considered, particularly the potential leaching of trace elements or residual compounds under field exposure conditions. Finally, pilot or small-scale field trials, along with life-cycle assessment (LCA) and life-cycle cost analysis (LCCA), are recommended to support the safe and sustainable implementation of PMMA-char in road construction.

CRediT authorship contribution statement

Chai Siah Lee: Writing – review & editing, Writing – original draft, Resources, Project administration, Methodology, Investigation, Formal analysis, Data curation, Conceptualization. **Lu Zhou:** Writing – review & editing, Writing – original draft, Resources, Project administration, Methodology, Investigation, Formal analysis, Data curation, Conceptualization. **Anand Sreeram:** Writing – review & editing, Supervision, Investigation. **Mohamed Adam:** Writing – review & editing, Formal analysis. **Ian Cardillo-Zallo:** Writing – review & editing, Formal analysis. **Edward Lester:** Writing – review & editing, Formal analysis. **Gordon Airey:** Writing – review & editing, Supervision, Funding acquisition, Conceptualization. **Eleanor Binner:** Writing – review & editing, Supervision, Project administration, Funding acquisition. **Derek Irvine:** Writing – review & editing, Supervision, Conceptualization.

Declaration of competing interest

The authors declare that they have no known competing financial interests or personal relationships that could have appeared to influence the work reported in this paper.

Acknowledgments

This work was supported by the Engineering and Physical Sciences Research Council [grant numbers EP/V038052/1 and EP/W000334/1], and Mitsubishi Chemical UK Ltd. The authors gratefully acknowledge all the support from Dr Jonathan Runnacles, Adam Clarke, Catherine Thompson, and Josh Walton from Mitsubishi Chemical UK Ltd. for providing the resources for this study and for sharing their invaluable insights and technical expertise, which supported and promoted the progress of this research. Furthermore, the authors would like to express gratitude to Eman Hussein, Jacob Ugana, and Adrian Quinn from the University of Nottingham for conducting the scanning electron microscope analysis, X-ray fluorescence analysis, and carbon and hydrogen elemental analysis, respectively. The authors would like to thank the Nanoscale and Microscale Research Centre and staff for access to instrumentation and technical support, under grant EP/W006413/1.

Appendix A. Supplementary data

Supplementary data to this article can be found online at https://doi.org/10.1016/j.jclepro.2026.148395.

Data availability

Data will be made available on request.

References

Avella, M., Errico, M.E., Martuscelli, E., 2001. Novel PMMA/CaCO3 nanocomposites abrasion resistant prepared by an in situ polymerization process. Nano Lett. 1, 213–217. https://doi.org/10.1021/nl015518v.

Bahraq, A.A., Al-Osta, M.A., Baghabra Al-Amoudi, O.S., Obot, I.B., Maslehuddin, M., Ahmed, H.-R., Saleh, T.A., 2022. Molecular simulation of cement-based materials and their properties. Engineering 15, 165–178. https://doi.org/10.1016/j.eng.2021.06.023.

Bhasin, A., Dallas, N.L., Rammohan, B., Vasconcelos, K., 2008. A framework to quantify the effect of healing in bituminous materials using material properties. Road Mater. Pavement Des. 9, 219–242. https://doi.org/10.1080/14680629.2008.9690167.

Braido, R.S., Borges, L.E.P., Pinto, J.C., 2018. Chemical recycling of crosslinked poly (methyl methacrylate) and characterization of polymers produced with the recycled monomer. J. Anal. Appl. Pyrolysis 132, 47–55. https://doi.org/10.1016/j.jaap.2018.03.017.

Bryant, P., 2005. Filler: is it “fixing” your binder?. In: AAPA Pavements Industry Conference. Surfers Paradise, Queensland.

Chaiyaput, S., Sertsoongnern, P., Ayawanna, J., 2022. Utilization of waste dust from asphalt concrete manufacturing as a sustainable subbase course material in pavement structures. Sustainability 14, 9804. https://doi.org/10.3390/su14169804.

Chen, W., Li, Y., Chen, S., Zheng, C., 2020. Properties and economics evaluation of utilization of oil shale waste as an alternative environmentally-friendly building materials in pavement engineering. Constr. Build. Mater. 259, 119698. https://doi.org/10.1016/j.conbuildmat.2020.119698.

Chen, Y., Xu, S., Tebaldi, G., Romeo, E., 2022. Role of mineral filler in asphalt mixture. Road Mater. Pavement Des. 23, 247–286. https://doi.org/10.1080/14680629.2020.1826351.

Chin, M.T., Yang, T., Quirion, K.P., Lian, C., Liu, P., He, J., Diao, T., 2024. Implementing a doping approach for poly(methyl methacrylate) recycling in a circular economy. J. Am. Chem. Soc. 146, 5786–5792. https://doi.org/10.1021/jacs.3c13223.

Cizer, Ö., Rodriguez-Navarro, C., Ruiz-Agudo, E., Elsen, J., Van Gemert, D., Van Balen, K., 2012. Phase and morphology evolution of calcium carbonate precipitated by carbonation of hydrated lime. J. Mater. Sci. 47, 6151–6165. https://doi.org/10.1007/s10853-012-6535-7.

Dimulescu, C., Burlacu, A., 2021. Industrial waste materials as alternative fillers in asphalt mixtures. Sustainability 13, 8068. https://doi.org/10.3390/su13148068.

Ding, Y., Zhang, W., Zhang, X., Han, D., Liu, W., Jia, J., 2022. Pyrolysis and combustion behavior study of PMMA waste from micro-scale to bench-scale experiments. Fuel 319, 123717. https://doi.org/10.1016/j.fuel.2022.123717.

Elimat, Z.M., Zihlif, A.M., Avella, M., 2008. Thermal and optical properties of poly (methyl methacrylate)/calcium carbonate nanocomposite. J. Exp. Nanosci. 3, 259–269. https://doi.org/10.1080/17458080802603715.

Gkaliou, K., Benedini, L., Sárossy, Z., Dalsgaard Jensen, C., Henriksen, U.B., Daugaard, A. E., 2023. Recycled PMMA prepared directly from crude MMA obtained from thermal depolymerization of mixed PMMA waste. Waste Manag. 164, 191–199. https://doi.org/10.1016/j.wasman.2023.04.007.

Hao, G., He, M., Lim, S.M., Ong, G.P., Zulkati, A., Kapilan, S., 2024. Recycling of plastic waste in porous asphalt pavement: engineering, environmental, and economic implications. J. Clean. Prod. 440, 140865. https://doi.org/10.1016/j.jclepro.2024.140865.

Holt, B.D., Engelkemeir, A.G., 1970. Thermal decomposition of barium sulfate to sulfur dioxide for mass spectrometric analysis. Anal. Chem. 42, 1451–1453. https://doi.org/10.1021/ac60294a032.

Hyun-Jong, L., Sias, D.J., Richard, K.Y., 2000. Continuum damage mechanics-based fatigue model of asphalt concrete. J. Mater. Civ. Eng. 12, 105–112. https://doi.org/10.1061/(ASCE)0899-1561(2000)12:2(105).

Kaminsky, W., Eger, C., 2001. Pyrolysis of filled PMMA for monomer recovery. J. Anal. Appl. Pyrolysis 58–59, 781–787. https://doi.org/10.1016/S0165-2370(00)00171-6.

Kandhal, Prithvi S., Chakraborty, Sanjoy, 1996. Effect of asphalt film thickness on short- and long-term aging of asphalt paving mixtures. Transp. Res. Rec. 1535, 83–90. https://doi.org/10.1177/0361198196153500111.

Karunadasa, K.S.P., Manoratne, C.H., Pitawala, H.M.T.G.A., Rajapakse, R.M.G., 2019. Thermal decomposition of calcium carbonate (calcite polymorph) as examined by in-situ high-temperature X-ray powder diffraction. J. Phys. Chem. Solid. 134, 21–28. https://doi.org/10.1016/j.jpcs.2019.05.023.

Kittipongvises, S., 2017. Assessment of environmental impacts of limestone quarrying operations in Thailand. Environmental and Climate Technologies 20, 67–83. https://doi.org/10.1515/rtuect-2017-0011.

Lawson, J.W., Srivastava, D., 2008. Formation and structure of amorphous carbon char from polymer materials. Phys. Rev. B 77, 144209. https://doi.org/10.1103/PhysRevB.77.144209.

Leng, Z., Padhan, R.K., Sreeram, A., 2018. Production of a sustainable paving material through chemical recycling of waste PET into crumb rubber modified asphalt. J. Clean. Prod. 180, 682–688. https://doi.org/10.1016/j.jclepro.2018.01.171.

Lesueur, D., Joëlle, P., Ritter, H.-J., 2013. The mechanisms of hydrated lime modification of asphalt mixtures: a state-of-the-art review. Road Mater. Pavement Des. 14, 1–16. https://doi.org/10.1080/14680629.2012.743669.

Li, F., Yang, Y., Wang, L., 2020. Evaluation of physicochemical interaction between asphalt binder and mineral filler through interfacial adsorbed film thickness. Constr. Build. Mater. 252, 119135. https://doi.org/10.1016/j.conbuildmat.2020.119135.

Li, S., Zhang, Z., Si, C., Shi, X., Cui, Y., Bao, B., Zhang, Q., 2025. Evaluation of the rheological properties of asphalt mastic incorporating iron tailings filler as an alternative to limestone filler. J. Clean. Prod. 486, 144444. https://doi.org/10.1016/j.jclepro.2024.144444.

Lin, P., Liu, X., Ren, S., Xu, J., Li, Y., Li, M., 2023. Effects of bitumen thickness on the aging behavior of high-content polymer-modified asphalt mixture. Polymers 15, 2325. https://doi.org/10.3390/polym15102325.

Little, D.N., Petersen, J.C., 2005. Unique effects of hydrated lime filler on the performance-related properties of asphalt cements: physical and chemical interactions revisited. J. Mater. Civ. Eng. 17, 207–218. https://doi.org/10.1061/(ASCE)0899-1561(2005)17:2(207).

Mihandoust, M., Ghabchi, R., 2025. Magnesium chloride deicer and asphalt: a multiscale approach to adhesion and damage characterisation. Road Mater. Pavement Des. 1–25. https://doi.org/10.1080/14680629.2025.2460469.

Miola, M., Lucchetta, G., Verné, E., 2023. Physical, mechanical, and biological properties of PMMA-based composite bone cement containing silver-doped bioactive and antibacterial glass particles with different particles sizes. Materials 16, 4499. https://doi.org/10.3390/ma16134499.

Mouillet, V., Séjourné, D., Delmotte, V., Ritter, H.-J., Lesueur, D., 2014. Method of quantification of hydrated lime in asphalt mixtures. Constr. Build. Mater. 68, 348–354. https://doi.org/10.1016/j.conbuildmat.2014.06.063.

Pipintakos, G., Sreeram, A., Mirwald, J., Bhasin, A., 2024. Engineering bitumen for future asphalt pavements: a review of chemistry, structure and rheology. Mater. Des. 244, 113157. https://doi.org/10.1016/j.matdes.2024.113157.

Ribeiro, H.J. da S., Ferreira, A.C., Ferreira, C.C., Pereira, L.M., Santos, M.C., Guerreiro, L. H.H., Assunção, F.P. da C., da Mota, S.A.P., Castro, D.A.R. de, Duvoisin, S., Borges, L. E.P., Machado, N.T., Bernar, L.P., 2024. Depolymerization of PMMA-based dental resin scraps on different production scales. Energies 17. https://doi.org/10.3390/en17051196.

Roberto, A., Bisanti, F., Pizzati, M., Mantovani, L., Romeo, E., Tebaldi, G., 2023. Stiffening effects of LFS slags reused as filler in asphalt mixtures. Constr. Build. Mater. 402, 132702. https://doi.org/10.1016/j.conbuildmat.2023.132702.

Russo, F., Veropalumbo, R., Oreto, C., Cassese, D., Papa, B., Malvezzi, S., 2022a. Reusing bottom ash as a filler from a waste-to-energy plant for making asphalt mastics. Case Stud. Constr. Mater. 17, e01406. https://doi.org/10.1016/j.cscm.2022.e01406.

Russo, F., Veropalumbo, R., Pontoni, L., Oreto, C., Biancardo, S.A., Viscione, N., Pirozzi, F., Race, M., 2022b. Sustainable asphalt mastics made up recycling waste as filler. J. Environ. Manag. 301, 113826. https://doi.org/10.1016/j.jenvman.2021.113826.

Santos, J.D.C., Brites, P., Martins, C., Nunes, C., Coimbra, M.A., Ferreira, P., Gonçalves, I., 2023. Starch consolidation of calcium carbonate as a tool to develop lightweight fillers for LDPE-based plastics. Int. J. Biol. Macromol. 226, 1021–1030. https://doi.org/10.1016/j.ijbiomac.2022.11.219.

Sasidharan, M., Eskandari Torbaghan, M., Burrow, M., 2019. Using Waste Plastics in Road Construction. Brighton, UK.

Sponchioni, M., Altinok, S., 2022a. Chapter seven - poly(methyl methacrylate): market trends and recycling. In: Moscatelli, D., Pelucchi, M. (Eds.), Advances in Chemical Engineering. Academic Press, pp. 269–287. https://doi.org/10.1016/bs.ache.2022.09.004.

Sponchioni, M., Altinok, S., 2022b. Chapter seven - poly(methyl methacrylate): market trends and recycling. In: Moscatelli, D., Pelucchi, M. (Eds.), Advances in Chemical Engineering. Academic Press, pp. 269–287. https://doi.org/10.1016/bs.ache.2022.09.004.

Taherkhani, H., Vahabi Kamsari, S., 2020. Evaluating the properties of zinc production wastes as filler and their effects on asphalt mastic. Constr. Build. Mater. 265, 120748. https://doi.org/10.1016/j.conbuildmat.2020.120748.

Wright, M., Parajuli, U., 2024. How Innovative Materials can Help Decarbonise England's Strategic Road Network. London.

Yang, B., Jiang, J., Wang, H., Leng, Z., Sui, X., Jiang, X., 2024. Optimization design of asphalt emulsion with rejuvenator towards a uniform distribution inside the damaged porous asphalt mixture for a better ravelling resistance. Case Stud. Constr. Mater. 21, e03747. https://doi.org/10.1016/j.cscm.2024.e03747.

Young, J.B., Hughes, R.W., Tamura, A.M., Bailey, L.S., Stewart, K.A., Sumerlin, B.S., 2023. Bulk depolymerization of poly(methyl methacrylate) via chain-end initiation for catalyst-free reversion to monomer. Chem 9, 2669–2682. https://doi.org/10.1016/j.chempr.2023.07.004.

Zhang, J., Liu, G., Zhu, C., Pei, J., 2017. Evaluation indices of asphalt–filler interaction ability and the filler critical volume fraction based on the complex modulus. Road Mater. Pavement Des. 18, 1338–1352. https://doi.org/10.1080/14680629.2016.1218789.

Zhang, R., Dai, Q., You, Z., Wang, H., Peng, C., 2018. Rheological performance of biochar modified asphalt with different particle sizes. Appl. Sci. 8, 1665. https://doi.org/10.3390/app8091665.

Zhao, Z., Wu, S., Liu, Q., Xie, J., Yang, C., Wan, P., Guo, S., Ma, W., 2021. Characteristics of calcareous sand filler and its influence on physical and rheological properties of asphalt mastic. Constr. Build. Mater. 301, 124112. https://doi.org/10.1016/j.conbuildmat.2021.124112.

Zhou, L., Gordon, A., Yuqing, Z., Wang, C., 2024. Multiscale characterisation on the adhesion and selective adsorption at bitumen–mineral interface. Road Mater. Pavement Des. 1–20. https://doi.org/10.1080/14680629.2024.2426012.